Can the observed enhancement in the mass spectrum of $p\bar{p}$ in $J/\psi \to \gamma p\bar{p}$ be interpreted by a possible $p\bar{p}$ bound state

Xiang Liu[1], Xiao-Qiang Zeng[1], Yi-Bing Ding[6,3], Xue-Qian Li[1,2,6], Hong Shen[1] and Peng-Nian Shen[5,4,2,6]

1. Department of Physics, Nankai University, Tianjin 300071, China

2. Institute of Theoretical Physics, CAS, P.O. Box 2735, Beijing, 100080, China

3. Graduate School of The Chinese Academy of Sciences, Beijing, 100039, China

4. Institute of High Energy Physics, CAS, P.O. Box 918(4), Beijing 100039, China

5. Center of Theoretical Nuclear Physics, National Laboratory of Heavy Ion Accelerator, Lanzhou 730000, China

6. China Center of Advanced Science and Technology (World Laboratory), P.O.Box 8730, Beijing 100080, China

Abstract

Provided the enhancement in the $p\bar{p}$ spectrum in radiative decay $J/\psi \to \gamma p\bar{p}$ observed by the BES collaboration is due to an existence of a $p\bar{p}$ molecular state, we calculate its binding energy and lifetime in the linear σ model. We consider a possibility that the enhancement is due to a $p\bar{p}$ resonance which is in either S-wave or P-wave structure and compare our results with the data.

1 Introduction

Recently, the BES collaboration has observed a near-threshold enhancement in the $p\bar{p}$ mass spectrum in the radiative decay $J/\psi \to \gamma p\bar{p}$ [1]. A similar report about the enhancement in $\bar{B^0} \to D^{*0} p\bar{p}$ and $B^{\pm} \to p\bar{p}K^{\pm}$ decays has been published by the Belle collaboration [2].

There have been various interpretations for the observed enhancement. The enhancement can be understood if the final state interaction between p and $\bar{p}$ is properly considered, as some authors suggested [3]. He et al. propose a possible mechanism that the final state of $\gamma p\bar{p}$ comes from an intermediate state of $\gamma + G$ where G is a 0^{-+} or 0^{++} glueball [4]. Meanwhile in analog to $a_0(980)$ and $f_0(980)$ which are supposed to be molecular states of $K\bar{K}$, it is tempted to assume that $p\bar{p}$ constitute a bound state with quantum number 0^{-+} or 0^{++}.

Under the assumption, one needs to evaluate the corresponding binding energy and lifetime, then compare the theoretical results with the data. In this work, we employ the linear σ model. Historically, there has been dispute about the linear σ model where the σ-meson stands as a realistic scalar meson [5] whereas in alternative scenarios, it is suggested that the contribution of σ can be attributed to two-pion exchange [6]. In fact, the difference between the linear σ model and non-linear σ model is whether the 0^{++} σ-meson is a substantial object, it corresponds to the linear or non-linear realization of the chiral lagrangian [7]. Because the low-energy QCD which is the underlying theory of hadron physics is fully non-perturbative, all the nonperturbative QCD parameters in the theory are so far not strictly derivable and have to be extracted by the data fitting. Therefore, determination of these parameters is somehow model-dependent and phenomenological. It is believed that at least for the leading order, all models would be applicable, even though they look somewhat different. As we employ the linear σ model which is simpler in calculations, we take all the coefficients by fitting data.

In our earlier work [8], we used the linear σ model to calculate the properties of deuteron, and by fitting data we not only determine the value of m_σ but also fix the corresponding parameters of the linear σ model. In this work we will use the same model with the parameters obtained by fitting the deuteron data to carry out all calculations for the $p\bar{p}$ bound state.

The present BES data do not finally decide if the resonance is an S-wave or P-wave bound state, but only indicate that the position of the S-wave peak is below the threshold $2m_p$ whereas the peak of the P-wave is a bit above the threshold. In our model, since the effective potential for the S-wave is attractive except a repulsive core near $r \to 0$, the binding energy must be negative, so that the calculated mass of the S-wave bound state is below the $2m_p$ threshold. Whereas for the P-wave due to the angular momentum barrier which is non-zero and positive, the binding energy becomes positive and the total mass is greater than $2m_p$.

To evaluate the widths for both S-wave and P-wave, we investigate the dissociation mechanism of the $p\bar{p}$ bound state. Since the central value of the mass of the S-wave bound state is smaller than $2m_p$, it dissolves into a $p\bar{p}$ pair via its width tail where the available energy is sufficient to produce a free $p\bar{p}$ pair. To evaluate the total width of the bound state, we need to achieve the imaginary part of the potential which is induced by the absorptive part of the loops in the $p\bar{p}$ elastic scattering amplitude (see the text for the concerned Feynman diagrams and some details). Thus according to the traditional method [9], we derive the real part of the potential which mainly comes from the tree-level scattering amplitude where t-channel mesons are exchanged, including σ, π, ρ and ω. For the S-wave bound state not only t-channel exchange, but also the s-channel annihilation contribute. Namely in the s-channel, η and η' are the intermediate mesons and they contribute a real part and an imaginary part to the effective potential, the s-channel contributions are proportional to a delta function $\delta(\mathbf{r})$ in the non-relativistic approximation. Thus the eigenenergy becomes $E_{Re} - i\frac{\Gamma}{2}$ and the time-factor is $exp(-iE_{Re}t - \frac{\Gamma}{2}t)$ and the Γ corresponds to the total width and $E_{Re} - i\frac{\Gamma}{2}$ is a solution of the Schrödinger equation with a complex potential.

For the P-wave, the binding energy is positive and the angular momentum barrier prevents dissociation of the bound state. It is noted that since $\psi(0) = 0$ for the P-wave, the imaginary part of the complex potential which is proportional to $\delta(\mathbf{r})$, does not result in an imaginary part to the eigenenergy. The dissolution mechanism of the bound state is the quantum tunnelling. By the WKB approximation method [10], the tunnelling transition proba-

bility is $exp[-2\int_a^b \sqrt{2\mu(V-E)}dr]$, thus the total width of the P-wave bound state would be $2\mu\, exp[-2\int_a^b \sqrt{2\mu(V-E)}dr]$, where $\mu = \frac{m_p}{2}$ is the reduced mass.

Substituting the potential no matter real and complex, into the Schrödinger equation, and solving it, one obtain both the eigenenergies and eigenfunctions of both S-wave and P-wave bound states. Then we can evaluate the masses and total widths of the bound states. That is the strategy of this work.

This paper is organized as follows. After this introduction, we derive the formulation for the complex potential with a brief introduction of the linear σ model. In sec. III, we substitute the potential into the Schrödinger equation and solve it to obtain the numerical result of the eigenenergy and eigenfunction, then obtain the masses and widths of the S- and P-wave bound states. In the section we also present all relevant parameters. The last section is devoted to our conclusion and discussion.

2 The formulation

(1) The necessary information about the model.

In the linear σ model, the effective Lagrangian is

$$L = g\bar{\psi}(\sigma + \gamma_5 \boldsymbol{\tau}\cdot\boldsymbol{\pi})\psi, \tag{1}$$

where ψ is the wavefunction of the nucleon. When we calculate the scattering amplitude, we introduce a form factor to compensate the off-shell effects of the exchanged mesons. At each vertex, the form factor is written as [8]

$$\frac{\Lambda^2 - M_m^2}{\Lambda^2 - q^2}, \tag{2}$$

where Λ is a phenomenological parameter and its value is near 1 GeV. It is observed that as $q^2 \to 0$ it becomes a constant and if $\Lambda \gg M_m$, it turns to be unity. In the case, as the distance is infinitely large, the vertex looks like a perfect point, so the form factor is simply 1 or a constant. Whereas, as $q^2 \to \infty$, the form factor approaches to zero, namely, in this situation, the distance becomes very small, the inner structure (quark, gluon degrees of freedom) would manifest itself and the whole picture of hadron interaction is no longer valid, so the form factor is zero which cuts off the end effects.

To derive an effective potential, one sets $q_0 = 0$ and writes down the elastic scattering amplitude in the momentum space and then carries out a Fourier transformation turning the amplitude into an effective potential in the configuration space. Following the standard procedure [9], we derive the effective potential from the scattering amplitude. Below, we present some details about the individual parts of the potential.

(2) The effective potentials.

(i) The real part of the potential.

Here we first consider the meson exchanges at the t-channel, because the intermediate meson is a space-like, it cannot be on its mass-shell, so that does not contribute to the imaginary part of the effective potential. Then we will go on discussing the s-channel contributions in subsection (ii).

a. Via exchanging π-meson:

The effective vertex is

$$L = g\bar{\psi}\gamma_5\boldsymbol{\tau}\cdot\boldsymbol{\pi}\psi, \tag{3}$$

and obviously only π^0 can be exchanged in our case.

The scattering amplitude in the momentum space is

$$V_\pi(\mathbf{q}) = -\frac{g_{NN\pi}^2}{4m^2(\mathbf{q}^2+m_\pi^2)}(\boldsymbol{\sigma}_1\cdot\mathbf{q})(\boldsymbol{\sigma}_2\cdot\mathbf{q})\left(\frac{\Lambda^2-m_\pi^2}{\Lambda^2+\mathbf{q}^2}\right)^2. \tag{4}$$

Following the standard procedure, we carry out a Fourier transformation on $V_\pi(\mathbf{q})$ and obtain the effective potential in the configuration space:

$$V_\pi(r) = \frac{g_{NN\pi}^2}{4m^2}(\boldsymbol{\sigma}_1\cdot\boldsymbol{\nabla})(\boldsymbol{\sigma}_2\cdot\boldsymbol{\nabla})f_\pi(r) \tag{5}$$

where

$$f_\pi(r) = \frac{e^{-m_\pi r}}{4\pi r} - \frac{e^{-\Lambda r}}{4\pi r} + \frac{(m_\pi^2-\Lambda^2)e^{-\Lambda r}}{8\pi\Lambda}. \tag{6}$$

b. Via σ and ρ and ω exchanges.

The effective vertices are respectively

$$L_\sigma = g\bar{\psi}\psi\sigma, \tag{7}$$

$$L_\rho = g_{_{NN}\rho}\bar{\psi}\gamma_\mu\tau^a\psi A^{a\mu}, \qquad a=1,2,3, \tag{8}$$

$$L_\omega = g_{_{NN}\omega}\bar{\psi}\gamma_\mu\psi\omega^\mu. \tag{9}$$

The scattering amplitude via exchanging σ-meson is

$$V_\sigma(\mathbf{q}) = \frac{g_{NN\sigma}^2}{4m^2(\mathbf{q}^2+m_\sigma^2)}[4m^2-4\mathbf{p}^2-\mathbf{q}^2-4(\mathbf{p}\cdot\mathbf{q})-i\boldsymbol{\sigma}\cdot(\mathbf{q}\times\mathbf{p})]\left(\frac{\Lambda^2-m_\sigma^2}{\Lambda^2+\mathbf{q}^2}\right)^2,$$

through a Fourier transformation, the potential is

$$V_\sigma(r) = \frac{g_{NN\sigma}^2}{4m^2}\Big[4m^2 f_\sigma(r) - 4\mathbf{p}^2 f_\sigma(r) + \boldsymbol{\nabla}^2 f_\sigma(r) + 4i(\mathbf{p}\cdot\mathbf{r})F_\sigma(r) - 2(\mathbf{L}\cdot\mathbf{S})F_\sigma(r)\Big],$$

where

$$f_\sigma(r) = \frac{e^{-m_\sigma r}}{4\pi r} - \frac{e^{-\Lambda r}}{4\pi r} + \frac{(m_\sigma^2-\Lambda^2)e^{-\Lambda r}}{8\pi\Lambda}$$

$$F_\sigma(r) = \frac{1}{r}\frac{\partial}{\partial r}f_\sigma(r).$$

Via exchanging vector-meson ρ(only ρ^0 contributes), the effective potential is

$$\begin{aligned} V_\rho(r) &= \frac{g_{NN\rho}^2}{4m^2}\Big[4m^2 f_\rho(r) - \boldsymbol{\nabla}^2 f_\rho(r) + 4\mathbf{p}^2 f_\rho(r) + 2(\mathbf{L}\cdot\mathbf{S})F_\rho(r) - 4i(\mathbf{p}\cdot\mathbf{r})F_\rho(r) \\ &\quad +(\boldsymbol{\sigma}_1\cdot\boldsymbol{\nabla})(\boldsymbol{\sigma}_2\cdot\boldsymbol{\nabla})f_\rho(r)\Big] \end{aligned}$$

where

$$\begin{aligned} f_\rho(r) &= \frac{e^{-m_\rho r}}{4\pi r} - \frac{e^{-\Lambda r}}{4\pi r} + \frac{(m_\rho^2-\Lambda^2)e^{-\Lambda r}}{8\pi\Lambda} \\ F_\rho(r) &= \frac{1}{r}\frac{\partial}{\partial r} f_\rho(r). \end{aligned}$$

For exchanging an ω vector meson, the expression is similar to that in the ρ case, but has an opposite sign to the ρ contribution due to the G-parity [21, 22], thus one only needs to replace the corresponding parameter values, such as the mass and coupling constant for ρ by that for ω and add a minus sign in front of all the terms of $V_\rho(r)$. For saving space, we dismiss the concrete expression for ω exchange.

c. The real part of the potential

A synthesis of all the individual contributions derived above stands as the real part of the effective potential, namely the traditional part of the effective potential as

$$\begin{aligned} V_{eff}(r) &= V_\pi(r) + V_\sigma(r) + V_\rho(r) + V_\omega(r) \\ &= V_0(r) + V_{LS}(r) + V_{pet}(r) + V_T + V_{SS}. \end{aligned}$$

In the expression the leading part of the potential is

$$\begin{aligned} V_0 &= \Big(\frac{e^{-\Lambda r}\Lambda g_{NN\sigma}^2}{8\pi} - \frac{e^{-\Lambda r} m_\sigma^2 g_{NN\sigma}^2}{8\pi\Lambda} + \frac{e^{-\Lambda r} g_{NN\sigma}^2}{4\pi r} - \frac{e^{-m_\sigma r} g_{NN\sigma}^2}{4\pi r}\Big) + \Big(-\frac{e^{-\Lambda r}\Lambda g_{NN\rho}^2}{8\pi} \\ &\quad + \frac{e^{-\Lambda r} m_\rho^2 g_{NN\rho}^2}{8\pi\Lambda} - \frac{e^{-\Lambda r} g_{NN\rho}^2}{4\pi r} + \frac{e^{-m_\rho r} g_{NN\rho}^2}{4\pi r}\Big) + \Big(\frac{e^{-\Lambda r}\Lambda g_{NN\omega}^2}{8\pi} - \frac{e^{-\Lambda r} m_\omega^2 g_{NN\omega}^2}{8\pi\Lambda} \\ &\quad + \frac{e^{-\Lambda r} g_{NN\omega}^2}{4\pi r} - \frac{e^{-m_\omega r} g_{NN\omega}^2}{4\pi r}\Big). \end{aligned}$$

The spin-orbit term is

$$\begin{aligned} V_{LS} &= \Big[\Big(\frac{e^{-\Lambda r} g_{NN\sigma}^2}{8m^2\pi r^3} - \frac{e^{-m_\sigma r} g_{NN\sigma}^2}{8m^2\pi r^3} + \frac{e^{-\Lambda r}\Lambda g_{NN\sigma}^2}{8m^2\pi r^2} - \frac{e^{-m_\sigma r} g_{NN\sigma}^2 m_\sigma}{8m^2\pi r^2} + \frac{e^{-\Lambda r}\Lambda^2 g_{NN\sigma}^2}{16m^2\pi r} \\ &\quad - \frac{e^{-\Lambda r} m_\sigma^2 g_{NN\sigma}^2}{16m^2\pi r}\Big) + \Big(\frac{e^{-\Lambda r} g_{NN\rho}^2}{8m^2\pi r^3} - \frac{e^{-m_\rho r} g_{NN\rho}^2}{8m^2\pi r^3} + \frac{e^{-\Lambda r}\Lambda g_{NN\rho}^2}{8m^2\pi r^2} - \frac{e^{-m_\rho r} m_\rho g_{NN\rho}^2}{8m^2\pi r^2} \\ &\quad + \frac{e^{-\Lambda r}\Lambda^2 g_{NN\rho}^2}{16m^2\pi r} - \frac{e^{-\Lambda r} m_\rho^2 g_{NN\rho}^2}{16m^2\pi r}\Big) + \Big(-\frac{e^{-\Lambda r} g_{NN\omega}^2}{8m^2\pi r^3} + \frac{e^{-m_\omega r} g_{NN\omega}^2}{8m^2\pi r^3} - \frac{e^{-\Lambda r}\Lambda g_{NN\omega}^2}{8m^2\pi r^2} \\ &\quad + \frac{e^{-m_\omega r} m_\omega g_{NN\omega}^2}{8m^2\pi r^2} - \frac{e^{-\Lambda r}\Lambda^2 g_{NN\omega}^2}{16m^2\pi r} + \frac{e^{-\Lambda r} m_\omega^2 g_{NN\omega}^2}{16m^2\pi r}\Big)\Big](\mathbf{L}\cdot\mathbf{S}). \end{aligned}$$

The relativistic correction which in our later numerical computations is treated as a perturbation to the leading part, is

$$
\begin{aligned}
V_{pet} &= \Big(\frac{e^{-\Lambda r}\Lambda^3 g_{NN\sigma}^2}{8m^2\pi} - \frac{e^{-\Lambda r}\Lambda m_\sigma^2 g_{NN\sigma}^2}{8m^2\pi} + \frac{e^{-\Lambda r} g_{NN\sigma}^2}{4m^2\pi r^3} - \frac{e^{-m_\sigma r} g_{NN\sigma}^2}{4m^2\pi r^3} + \frac{e^{-\Lambda r}\Lambda g_{NN\sigma}^2}{4m^2\pi r^2} \\
&\quad - \frac{e^{-m_\sigma r} m_\sigma g_{NN\sigma}^2}{4m^2\pi r^2} + \frac{e^{-\Lambda r}\Lambda^2 g_{NN\sigma}^2}{8m^2\pi r} + \frac{e^{-\Lambda r} m_\sigma^2 g_{NN\sigma}^2}{8m^2\pi r} - \frac{e^{-m_\sigma r} m_\sigma^2 g_{NN\sigma}^2}{4m^2\pi r}\Big) \\
&\quad + \Big(\frac{3e^{-\Lambda r}\Lambda^3 g_{NN\rho}^2}{32m^2\pi} - \frac{3e^{-\Lambda r}\Lambda m_\rho^2 g_{NN\rho}^2}{32m^2\pi} + \frac{e^{-\Lambda r} g_{NN\rho}^2}{4m^2\pi r^3} - \frac{e^{-m_\rho r} g_{NN\rho}^2}{4m^2\pi r^3} + \frac{e^{-\Lambda r} g_{NN\rho}^2\Lambda}{4m^2\pi r^2} \\
&\quad - \frac{e^{-m_\rho r} g_{NN\rho}^2 m_\rho}{4m^2\pi r^2} + \frac{e^{-\Lambda r}\Lambda^2 g_{NN\rho}^2}{8m^2\pi r} + \frac{e^{-\Lambda r} m_\rho^2 g_{NN\rho}^2}{16m^2\pi r} - \frac{3e^{-m_\rho r} m_\rho^2 g_{NN\rho}^2}{16m^2\pi r}\Big) \\
&\quad + \Big(-\frac{3e^{-\Lambda r}\Lambda^3 g_{NN\omega}^2}{32m^2\pi} + \frac{3e^{-\Lambda r}\Lambda m_\omega^2 g_{NN\omega}^2}{32m^2\pi} - \frac{e^{-\Lambda r} g_{NN\omega}^2}{4m^2\pi r^3} + \frac{e^{-m_\omega r} g_{NN\omega}^2}{4m^2\pi r^3} - \frac{e^{-\Lambda r} g_{NN\omega}^2\Lambda}{4m^2\pi r^2} \\
&\quad + \frac{e^{-m_\omega r} g_{NN\omega}^2 m_\omega}{4m^2\pi r^2} - \frac{e^{-\Lambda r}\Lambda^2 g_{NN\omega}^2}{8m^2\pi r} - \frac{e^{-\Lambda r} m_\omega^2 g_{NN\omega}^2}{16m^2\pi r} + \frac{3e^{-m_\omega r} m_\omega^2 g_{NN\omega}^2}{16m^2\pi r}\Big).
\end{aligned}
$$

The tensor potential is

$$
\begin{aligned}
V_T &= \Big(\frac{e^{-\Lambda r}\Lambda^3 g_{NN\pi}^2}{96m^2\pi} - \frac{e^{-\Lambda r}\Lambda m_\pi^2 g_{NN\pi}^2}{96m^2\pi} + \frac{e^{-\Lambda r} g^2}{16m^2\pi r^3} - \frac{e^{-m_\pi r} g_{NN\pi}^2}{16m^2\pi r^3} + \frac{e^{-\Lambda r}\Lambda g_{NN\pi}^2}{16m^2\pi r^2} r \\
&\quad - \frac{e^{-m_\pi r} m_\pi g_{NN\pi}^2}{16m^2\pi r^2} + \frac{e^{-\Lambda r}\Lambda^2 g_{NN\pi}^2}{32m^2\pi r} - \frac{e^{-\Lambda r} m_\pi^2 g_{NN\pi}^2}{96m^2\pi r} - \frac{e^{-m_\pi r} m_\pi^2 g_{NN\pi}^2}{48m^2\pi r}\Big) \\
&\quad + \Big(-\frac{e^{-\Lambda r}\Lambda^3 g_{NN\rho}^2}{96m^2\pi} + \frac{e^{-\Lambda r}\Lambda m_\rho^2 g_{NN\rho}^2}{96m^2\pi} - \frac{e^{-\Lambda r} g_{NN\rho}^2}{16m^2\pi r^3} + \frac{e^{-m_\rho r} g_{NN\rho}^2}{16m^2\pi r^3} - \frac{e^{-\Lambda r}\Lambda g_{NN\rho}^2}{16m^2\pi r^2} \\
&\quad + \frac{e^{-m_\rho r} m_\rho g_{NN\rho}^2}{16m^2\pi r^2} - \frac{e^{-\Lambda r}\Lambda^2 g_{NN\rho}^2}{32m^2\pi r} + \frac{e^{-\Lambda r} m_\rho^2 g_{NN\rho}^2}{96m^2\pi r} + \frac{e^{-m_\rho r} m_\rho^2 g_{NN\rho}^2}{48m^2\pi r}\Big) \\
&\quad + \Big(\frac{e^{-\Lambda r}\Lambda^3 g_{NN\omega}^2}{96m^2\pi} - \frac{e^{-\Lambda r}\Lambda m_\omega^2 g_{NN\omega}^2}{96m^2\pi} + \frac{e^{-\Lambda r} g_{NN\omega}^2}{16m^2\pi r^3} - \frac{e^{-m_\omega r} g_{NN\omega}^2}{16m^2\pi r^3} \\
&\quad + \frac{e^{-\Lambda r}\Lambda g_{NN\omega}^2}{16m^2\pi r^2} - \frac{e^{-m_\omega r} m_\omega g_{NN\omega}^2}{16m^2\pi r^2} + \frac{e^{-\Lambda r}\Lambda^2 g_{NN\omega}^2}{32m^2\pi r} - \frac{e^{-\Lambda r} m_\omega^2 g_{NN\omega}^2}{96m^2\pi r} \\
&\quad - \frac{e^{-m_\omega r} m_\omega^2 g_{NN\omega}^2}{48m^2\pi r}\Big)\Big[\frac{3(\boldsymbol{\sigma}_1\cdot\mathbf{r})(\boldsymbol{\sigma}_2\cdot\mathbf{r})}{r^2} - (\boldsymbol{\sigma}_1\cdot\boldsymbol{\sigma}_2)\Big],
\end{aligned}
$$

and the spin-spin term is

$$
\begin{aligned}
V_{SS} &= \Big(\frac{e^{-\Lambda r}\Lambda^3 g_{NN\pi}^2}{96m^2\pi} - \frac{e^{-\Lambda r}\Lambda m_\pi^2 g_{NN\pi}^2}{96m^2\pi} + \frac{e^{-\Lambda r} m_\pi^2 g_{NN\pi}^2}{48m^2\pi r} - \frac{e^{-m_\pi r} m_\pi^2 g_{NN\pi}^2}{48m^2\pi r}\Big) \\
&\quad + \Big(\frac{e^{-\Lambda r}\Lambda^3 g_{NN\rho}^2}{48m^2\pi} - \frac{e^{-\Lambda r}\Lambda m_\rho^2 g_{NN\rho}^2}{48m^2\pi} + \frac{e^{-\Lambda r} m_\rho^2 g_{NN\rho}^2}{24m^2\pi r} - \frac{e^{-m_\rho r} m_\rho^2 g_{NN\rho}^2}{24m^2\pi r}\Big) \\
&\quad + \Big(-\frac{e^{-\Lambda r}\Lambda^3 g_{NN\omega}^2}{48m^2\pi} + \frac{e^{-\Lambda r}\Lambda m_\omega^2 g_{NN\omega}^2}{48m^2\pi} - \frac{e^{-\Lambda r} m_\omega^2 g_{NN\omega}^2}{24m^2\pi r} \\
&\quad + \frac{e^{-m_\omega r} m_\omega^2 g_{NN\omega}^2}{24m^2\pi r}\Big)(\boldsymbol{\sigma}_1\cdot\boldsymbol{\sigma}_2).
\end{aligned}
$$

d. The case of $p\bar{p}$ is different from the deuteron where the constituents are p and n, namely there is a $p\bar{p}$ annihilation at the s-channel, which would contribute a delta function to the effective potential.

If $p\bar{p}$ is in S-wave with quantum number $I^GJ^{PC} = 0^+(0^{-+})$, in the s-channel only a $0^+(0^{-+})$ meson can be exchanged. Here we only consider the lowest-lying pseudoscalar mesons of 0^{-+} η and η'. Their contribution can be written as

$$V_\eta^{'}(r) = \frac{g_{NN\eta}^2}{(4m^2-m_\eta^2)}\Big(\frac{\Lambda^2-m_\eta^2}{4m^2-\Lambda^2}\Big)^2\Big[-1+\frac{(\boldsymbol{\sigma}_1\cdot\boldsymbol{\nabla})(\boldsymbol{\sigma}_2\cdot\boldsymbol{\nabla})}{2m^2}-\frac{\boldsymbol{\nabla}^2}{2m^2}\Big]\delta^3(\mathbf{r}),$$

where m is the invariant mass $\sqrt{(p_1+p_2)^2}$ and $p_1,\ p_2$ are the four-momenta of the constituents p and $\bar{p}$ respectively, and it is very close to $2m_p$. For the contribution of η', one only needs to replace the corresponding parameters values. It is noted that these contributions still belong to the real part of the effective potential. Below, we will derive the imaginary contributions induced by the absorptive part of loops at s-channel.

(ii) The imaginary part of the complex potential.

The corresponding Feynman diagrams are shown in Figs.1 and 2. Fig.1 is the self-energy of η and η' which are off-shell and Fig.2 is a box diagram. Obviously, the elastic scattering of $p\bar{p}$ is a strong-interaction process, so that parity, isospin etc. quantum numbers must be conserved and as long as the $p\bar{p}$ bound state is of the 0^{-+} structure, only η and η' can be exchanged in the s-channel (we neglect higher-resonances).

The concerned couplings are [11, 12, 13]

$$L_{PP\sigma} = -\frac{\gamma_{PP\sigma}}{\sqrt{2}}\sigma\partial_\mu\boldsymbol{P}\cdot\partial_\mu\boldsymbol{P}, \tag{10}$$

$$L_{VVp} = g_{VVp}\varepsilon^{\mu\nu\lambda\sigma}\partial_\mu V_\nu(\boldsymbol{P}\cdot\partial_\lambda\boldsymbol{V}_\sigma), \tag{11}$$

here $\mathbf{P}$ stands as pseudoscalar mesons, such as π, η and η' etc. and $\mathbf{V}$ denotes vector mesons, such as ω and ρ etc.

The imaginary part of the potential is obtained in the following way. First, we calculate the absorptive part of the loops by the Cutkosky cutting rule in the momentum space [14] and carry out a Fourier transformation turning it into an imaginary part of the complex potential.

(i) The contribution induced by the self-energy of η and η'.

We have obtained

$$V_{\mathbf{Im}_1}(r) = -\frac{\gamma_{\eta\eta\sigma}^2 g_{NN\eta}^2(4m^2-m_\sigma^2+m_\eta^2)^2}{512\pi m^2(4m^2-m_\eta^2)^2}\sqrt{-16m^2m_\eta^2+(4m^2-m_\sigma^2+m_\eta^2)^2},$$
$$\times\Big(\frac{\Lambda^2-m_\eta^2}{4m^2-\Lambda^2}\Big)^2\delta^3(\mathbf{r}), \qquad \text{for Fig.1(a).}$$

$$V_{\mathbf{Im}_2}(r) = -\frac{\gamma_{\eta\eta f_0}^2 g_{NN\eta}^2(4m^2-m_{f_0}^2+m_\eta^2)^2}{512\pi m^2(4m^2-m_\eta^2)^2}\sqrt{-16m^2m_\eta^2+(4m^2-m_{f_0}^2+m_\eta^2)^2}$$
$$\times\Big(\frac{\Lambda^2-m_\eta^2}{4m^2-\Lambda^2}\Big)^2\delta^3(\mathbf{r}), \qquad \text{for Fig.1(b).}$$

$$V_{\mathbf{Im}_3}(r) = -\frac{\gamma^2_{\pi\eta a_0} g^2_{NN\eta}(4m^2 - m^2_{a_0} + m^2_\pi)^2}{512\pi m^2(4m^2 - m^2_\eta)^2}\sqrt{-16m^2m^2_\pi + (4m^2 - m^2_{a_0} + m^2_\pi)^2}$$
$$\times\Big(\frac{\Lambda^2 - m^2_\eta}{4m^2 - \Lambda^2}\Big)^2\delta^3(\mathbf{r}), \qquad \text{for Fig.1(c).}$$

and

$$V_{\mathbf{Im}_4}(r) = -\frac{g^2_{\eta\rho\rho}g^2_{NN\eta}(16m^4 - 4m^2m^2_\rho)}{128\pi m^2(4m^2 - m^2_\eta)^2}\sqrt{16m^4 - 16m^2m^2_\rho}\Big(\frac{\Lambda^2 - m^2_\eta}{4m^2 - \Lambda^2}\Big)^2\delta^3(\mathbf{r}), \qquad \text{for Fig.1(d).}$$

b. The contributions induced by the box diagram

$$V_{\mathbf{Im}_{box}}(\mathbf{p}) = 2g^2_{NN\sigma}g^2_{NN\eta}\int\frac{d^4q}{(2\pi)^4}\overline{v}(p_2)\frac{\not{p}_1 - \not{q} + m}{(p_1 - q)^2 - m^2}\gamma^5 u(p_1)\overline{u}(p_3)\gamma^5\frac{\not{p}_3 - \not{q} + m}{(p_3 - q)^2 - m^2}v(p_4)$$
$$\times(i\pi)^2\delta(q^2 - m^2_\eta)\delta([p_1 + p_2 - q]^2 - m^2_\sigma)\Big(\frac{\Lambda^2 - m^2}{(p_1 - q)^2 - \Lambda^2}\Big)^2\Big(\frac{\Lambda^2 - m^2}{(p_3 - q)^2 - \Lambda^2}\Big)^2.$$

Taking the Fourier transformation, we obtain

$$V_{\mathbf{Im}_{box}}(r) = \int_0^\pi\Big\{\frac{g^2_{NN\sigma}g^2_{NN\eta}\mathcal{B}(\Lambda^2 - m^2)^4}{16\pi\mathcal{A}[\mathcal{A}^2 - \mathcal{B}^2 - 2(\mathcal{A}\sqrt{m^2 + \mathbf{p}^2} - \mathcal{B}\mathbf{p}\cos(\theta))]^2}$$
$$\times\frac{[-m^2 - (m + \frac{\mathbf{p}^2}{2m} - \mathcal{A})^2 + 2m(m + \frac{\mathbf{p}^2}{2m} - \mathcal{A})]Sin(\theta)}{[m^2 - \mathcal{B}^2 + \mathcal{A}^2 - \Lambda^2 - 2(\mathcal{A}\sqrt{m^2 + \mathbf{p}^2} - \mathcal{B}\mathbf{p}\cos(\theta))]^4}\Big\}d\theta\delta^3(\mathbf{r}),$$

where

$$\mathcal{A} = \sqrt{m^2_\eta + \mathcal{B}^2},$$

and

$$\mathcal{B} = \frac{1}{4}\sqrt{16m^2 - 8m^2_\eta - 8m^2_\sigma + 16\mathbf{p}^2 + \frac{m^4_\eta}{m^2 + \mathbf{p}^2} - \frac{2m^2_\eta m^2_\sigma}{m^2 + \mathbf{p}^2} + \frac{m^4_\sigma}{m^2 + \mathbf{p}^2}}.$$

Expanding the expression with respect to $|\mathbf{p}|$ and keeping terms up to $\mathbf{p}^2$, we have the final expression as

$$V_{\mathbf{Im}_{box}}(r) = \Big[\frac{-g^2_{NN\sigma}g^2_{NN\eta}(4m^2 - m^2_\sigma + m^2_\eta)^2(m^2 - \Lambda^2)^4}{16\pi m^4(-4m^2 + m^2_\sigma + m^2_\eta)^2(-2m^2 + m^2_\sigma + m^2_\eta - 2\Lambda^2)^4}$$
$$\times\sqrt{16m^4 + (m^2_\eta - m^2_\sigma)^2 - 8m^2(m^2_\eta + m^2_\sigma)^2} + \mathcal{O}(m, m_\sigma, m_\eta, , \Lambda)\mathbf{p}^2\Big]\delta^3(\mathbf{r})$$

where the coefficient $\mathcal{O}(m, m_\sigma, m_\eta, \Lambda)$ of $\mathbf{p}^2$ is obtained by a tedious but straightforward calculation, here for saving space we ignore the details.

Finally we obtain the imaginary part of the potential as

$$V_{\mathbf{Im}}(r) = V_{\mathbf{Im}_1}(r) + V_{\mathbf{Im}_2}(r) + V_{\mathbf{Im}_3}(r) + V_{\mathbf{Im}_4}(r) + V_{\mathbf{Im}_{box}}(r).$$

It is also noted that for the P-wave resonance, the wavefunction at origin is zero, i.e. $\psi(0) = 0$, at the leading order there is no s-channel contribution to the effective potential, and neither the imaginary part in the final effective potential, since in our approximation, all of them are proportional to $\delta^3(\mathbf{r})$.

In the practical computation, a popular approximation [15] for the delta function

$$\delta^3(\mathbf{r}) \propto \frac{\alpha^3}{\pi^{\frac{3}{2}}} e^{-\alpha^2 r^2}$$

is adopted.

3 Numerical results

By solving the Schrödinger equation, we obtain the zero-th order engenenergy and wavefunction, where the L-S coupling and tensor terms are taken as perturbations and the imaginary part of the complex potential is treated in two ways. In terms of the traditional method of Quantum Mechanics, we can calculate the corrections.

For the S-wave resonance we obtain the binding energy and the total width as

m_σ(GeV)	0.47	0.48	0.49	0.50	0.51	0.52	0.53	0.54	0.55
Λ(GeV)	0.59	0.60	0.61	0.62	0.63	0.64	0.65	0.66	0.67
Es(MeV)	-18.38	-17.23	-16.19	-15.30	-14.47	-13.67	-13.03	-12.42	-11.88
Γ_s(MeV)	33.60	30.08	26.94	24.15	21.67	19.49	17.57	15.90	14.45

Table 1: the theoretical results for the S-wave with perturbative method

The number listed in table.1 are obtained in terms of the perturbation method. Namely, we take the imaginary part of the complex potential as a perturbation as well as the L-S coupling and tensor terms,

$$\Delta E = < \psi_0 | \Delta H | \psi_0 >,$$

where $\Delta H = \Delta H_{real} + i\Delta H_{imag}$ and ψ_0 is the wavefunction of zero-th order.

As we sandwich the imaginary part of the complex potential between ψ_0, the expectation value is the imaginary part of the complex eigenenergy as

$$i\Delta E_{imag} = -i\frac{\Gamma}{2} = < \psi_0 | iV_{\mathbf{Im}}(r) | \psi_0 >,$$

and

$$iV_{\mathbf{Im}}(r) \equiv i\Delta H_{imag}.$$

Thus the total eigenenergy is

$$E = E_0 + \Delta E_{real} + i\Delta E_{imag} = E_0 + \Delta E_{real} - i\frac{\Gamma}{2}.$$

Instead, one can solve the Schrödinger equation with a complex potential which would be divided into two coupled differential equations. The coupled equations cannot, in general, be solved analytically, but only numerically. We obtain the complex eigenenergy by solving the equation group and the results are listed in table 2.

m_σ(GeV)	0.47	0.48	0.49	0.50	0.51	0.52	0.53	0.54	0.55
Λ(GeV)	0.59	0.60	0.61	0.62	0.63	0.64	0.65	0.66	0.67
Es(MeV)	-14.10	-13.64	-13.17	-12.71	-12.25	-11.81	-11.38	-10.99	-10.62
Γ_s(MeV)	21.90	19.48	17.29	15.29	13.48	11.87	10.45	9.19	8.11

Table 2: the calculated results for the S-wave with direct program calculating

Comparing the results in table 1 and 2, we find that there are some deviations of no more than 30%, and generally, the numbers obtained in the perturbation method are a bit greater than them by directly solving the coupled equations, but qualitatively, the two sets are consistent. Considering the experimental errors and theoretical uncertainties, we would conclude that the two sets of numbers agree with each other.

For the P-wave, by solving the Schrödinger equation, we obtain the eigenenergy, and then by the WKB method, we can estimate the dissociation rate, which turns out to be the width of the P-wave resonance. The results are shown in Table 2.

m_σ(GeV)	0.47	0.48	0.49	0.50	0.51	0.52	0.53	0.54	0.55
$\Lambda(\times 10^{-1}$ GeV)	8.25	8.51	8.76	9.02	9.28	9.54	9.81	10.08	10.35
Ep(MeV)	0.35	0.43	0.54	0.63	0.72	0.80	0.87	0.94	1.08
Γ_p(MeV)	9.11	11.42	15.00	17.96	20.22	22.64	24.26	25.91	29.98

Table 3: The calculated values for P-wave

For the theoretical calculations, we have employed the following parameters as inputs: $m = 0.938$(GeV); $m_\pi = 0.138$(GeV); $m_\rho = 0.77$(GeV); $m_\omega = 0.783$(GeV); $m_\eta = 0.547$(GeV); $m_{\eta'} = 0.958$(GeV); $m_{f_0} = 0.98$(GeV); $m_{a_0} = 0.98$(GeV) [16]; $g_{NN\pi} = g_{NN\sigma} = 13.5$; $g_{NN\rho} = g_{NN\omega} = 3.25$ [17]; $\frac{g^2_{NN\eta}}{4\pi} = 0.4$; $\frac{g^2_{NN\eta'}}{4\pi} = 0.6$ [18]; $\gamma_{\eta\eta\sigma} = 4.11(\text{GeV}^{-1})$; $\gamma_{\eta\eta'\sigma} = 2.65(\text{GeV}^{-1})$; $\gamma_{\eta\eta f_0} = 1.72(\text{GeV}^{-1})$; $\gamma_{\eta\eta' f_0} = -9.01(\text{GeV}^{-1})$; $\gamma_{\pi\eta a_0} = -6.80(\text{GeV}^{-1})$; $\gamma_{\pi\eta' a_0} = -7.80(\text{GeV}^{-1})$ [19]; $g_{\eta\rho\rho} = -16(\text{GeV}^{-1})$[13][20].

4 Conclusion and discussion

In this work, in terms of the linear σ model we investigate the spectrum and total width of the possible $p\bar{p}$ bound states. We consider two possibilities that the observed enhancement is due to a $p\bar{p}$ bound state in S- or P-waves respectively.

All the parameters employed in the calculations were obtained by fitting the data of deuteron. With the very precise measurement on the binding energy of deuteron and more or less accurate estimate of the s-d mixing and charge radius, there is only a narrow window in the parameter space [8]. Namely there is almost not much free room to adjust them, and neither is a large range for changing our theoretical calculations, as long as the model is employed. Therefore the newly observed resonance, if it is experimentally confirmed, can also provide an opportunity to further testify the linear σ model.

We derive the effective potential between p and $\bar{p}$, and for the S-wave structure, we simply substitute it into the schrödinger equation to obtain the binding energy. We have also calculated the absorptive part of the concerned loops by the Cutkosky cutting rule and it becomes the imaginary part of the potential. Differently from the deuteron case which is a bound state of pn, for the $p\bar{p}$ case, there exist s-channel processes (see the figures in the text), which can contribute a real part (the tree level meson exchange) to the potential and an imaginary part through the loop diagrams in the channel and both of them are proportional to $\delta(\mathbf{r})$ at the concerned non-relativistic approximation. In this work, we ignore the dispersive part of the loops because it depends on the renormalization scheme and only makes a correction to the leading contribution of the real part of the potential, but keep the absorptive part which is the only source of the imaginary part of the potential.

When we solve the Schrödinger equation with a complex potential, we have taken certain approximations to simplify the calculations. Then we obtain the mass and total width of the S-wave resonance.

It is also noted that due to the G-parity structure of the NN and $N\bar{N}$ systems where N refers to nucleons, the potentials contributed by σ and ρ are of the same sign for the NN and $N\bar{N}$ systems, but the potential induced by π^0 and ω should have opposite signs for the two systems [21, 22]. In fact, for the deuteron case, which is in the pn structure, the contribution of π^0 is repulsive, and so is that from ρ and ω. But for the $p\bar{p}$ system, π^0 and ω induce attractive potentials while the contribution induced by σ and ρ remain unchanged. It can qualitatively explain why the the binding energy for $p\bar{p}$ (about -18 MeV) is more negative than that for deuteron (about -2.22 MeV).

For the P-wave case, where the wave function of origin is zero, i.e. $\psi(0) = 0$, one does not need to calculate the s-channel contribution. The angular momentum barrier prevents dissociation of the bound state, but the quantum tunnelling leads to a final dissolution of the bound state and this tunnelling rate determines the total width or lifetime of the P-wave bound state of $p\bar{p}$. Fig.3 shows the effective potential for S-wave and P-wave respectively. The repulsive part at the region of small r is due to the vector-meson exchange. One also notes that for the S-wave, besides the repulsive core for small r the potential is attractive, whereas for the P-wave, there exists an angular barrier which results in an positive binding energy, i.e. the total mass of the P-wave resonance is above the threshold of $2m_p$. Since the barrier is not high, the binding energy is not far above zero and the total mass is very close to $2m_p$. To evaluate the tunnelling rate we use the WKB method, however, since the barrier is not much higher than the binding energy level, using the WKB method might bring up certain errors. Therefore the estimated width can only be valid to its order of magnitude. Indeed, with present experimental accuracy, we can satisfy ourselves with such numbers, but definitely the future experiments can provide us with much more information and by them we will modify our model and determine the concerned

parameters to higher accuracy.

The newly observed enhancement by BES and Belle may have various interpretations, one of them is due to a resonance of $p\bar{p}$. In this work we discuss this possibility in the linear $\sigma-$model and the obtained values are quantitatively consistent with the data. Our numerical results show, the total width and position of the proposed bound state, no matter S-wave or P-wave do not contradict the data, therefore both of them may be possible states which can accommodate the observed enhancement.

The authors of [3] suggested an alternative explanation, i.e. the final state interaction results in the observed enhancement. To decide which mechanism is right or dominant would wait for the future experiments. We hope that studies on the new resonance can enrich our knowledge about the hadron physics and the interactions at the hadron level. Our conclusion is that to confirm the observed enhancement, more precise measurements are needed.

Acknowledgment:

We thank K.T. Chao for his helpful comments and suggestions, we also benefit from the fruitful discussions with C.H. Chang. This work is partially supported by the National Natural Science Foundation of China.

References

[1] J.Z. Bai et al., Phys. Rev. Lett. **91** (2003) 022001.

[2] K. Abe et al., Phys. Rev. Lett. **88** (2002) 181803; **89** (2002) 151802.

[3] B.S. Zou and H.C. Chiang, Phys. Rev. D69 (2004) 034004; B. Kerbikov, A. Stavinsky and V. Fedotov, hep-ph/0402054;

[4] X.G. He et al., in preparetion.

[5] H. Georgi, *Weak Interactions and Modern Particle Theory*, The Benjamin/Cummings Pub.Co. (1984), New York.

[6] R. Machleidt, K. Holinde and Ch. Elster, Phys. Rep. **149**, No. 1 (1987).

[7] Y.B. Dai and Y.L. Wu, Eur. Phys. J. C (2004) (DOI) 10.1140/epjcd/s2004-01-001-3.

[8] Yi-Bing Ding et al., hep-ph/0402109.

[9] V. Benresteskii, E. Lifshitz and L. Pitaeevskii, *Quantum Electrodynamics*, Pergamon Press, 1982, New York.

[10] S. Gasiorowicz, *Quantum Mechanics*, 2nd ed., Wiley, 1995, New York.

[11] Masayasu Harada, hep-ph/9606331; F. Sannino and J. Schechter, Phys. Rev. **D52** (1995) 96-107; D. Black et al., Phys. Rev. **D58** (1998) 054012.

[12] N.N. Achasov and A.A. Kozhevnikov, Phys. Rev. **D62** (2000) 056011.

[13] J.L. Lucio, M. Napsuciale, M.D. Scadron and V.M. Villanueva, hep-ph/9902349; A. Gokalp, A. Kucukarslan, S. Solmaz, O. Yilmaz, Acta Phys. Polon. **B34** (2003) 4095-4104; J. Wess and B. Zumino, Phys. Lett. **B37** (1971) 65.

[14] See e.g., C. Itzykson and J.B. Zuber, Quantum Field Theory, McGrow-Hill, 1980, New York.

[15] W. Lucha, F.F. Schöberl and D. Gromes, Phys. Rep. **200**, No. 4 (1991) 127-240.

[16] The Data Group, Eur. Phys. J. **C15** (2000) 1.

[17] Z. Lin et al. Phys. Rev. **C61** (2000) 024904; B. Holzenkamp et al. Nucl. Phys. **A500** (1989) 485; G. Janssen et al. Phys. Rev. Lett. **71** (1993) 1975.

[18] L. Tiator, C. Bennhold and S.S. Kamalov, Nucl. Phys. **A580** (1994) 455-474.

[19] Deirdre Black, Amir H. Fariborz and Joseph Schechter, Phys. Rev. **D61** (2000) 074030.

[20] M. Lublinsky, Phys. Rev. **D55** (1997) 249-254.

[21] E. Klempt, F. Bradamante, A. Martin and J. Richard, Phys. Rep. **368** (2002) 119-316.

[22] Jean-Marc Richard, Nucl. Phys. Proc. Suppl, **86** (2000) 361.

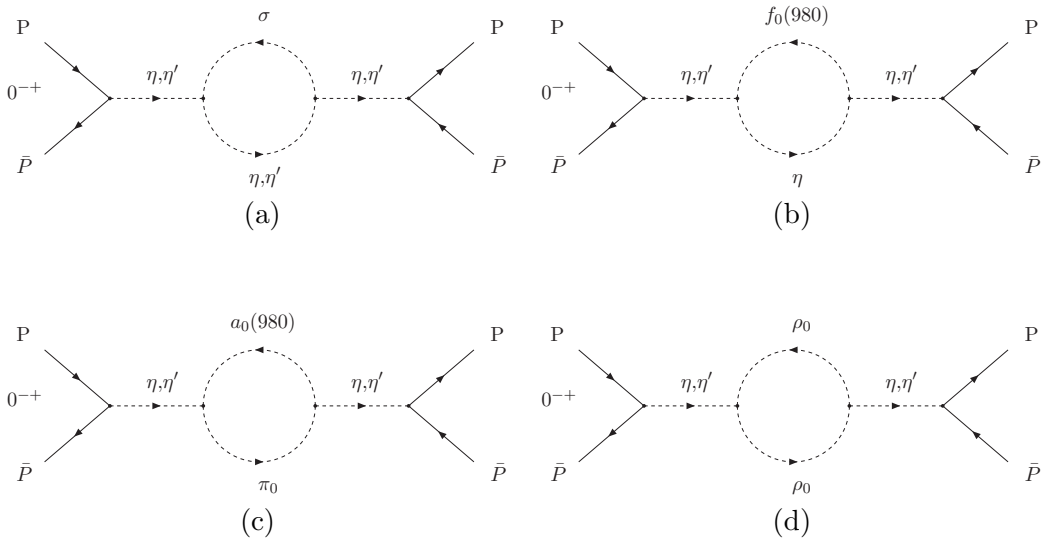

Figure 1:

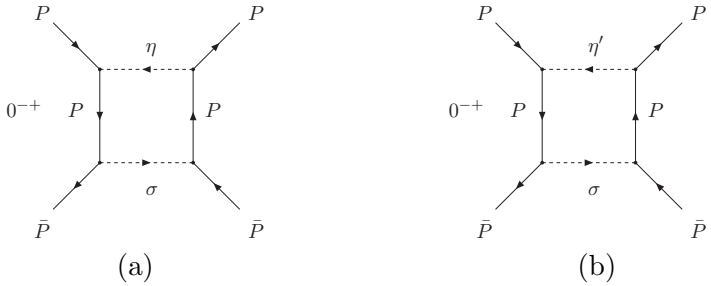

Figure 2:

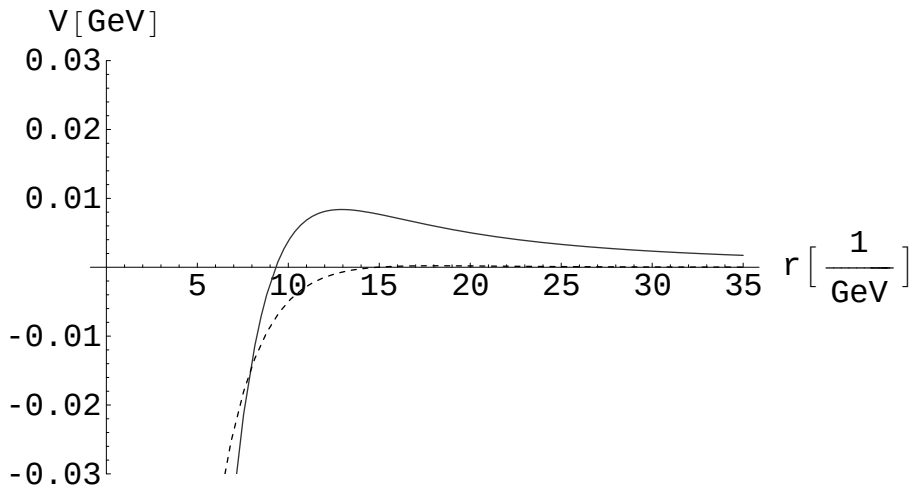

Figure 3: